

This is a postprint version of the following published document:

Bustos, A., Rubio, H., Castejon, C. & Garcia-Prada, J. C. (2019). Condition monitoring of critical mechanical elements through Graphical Representation of State Configurations and Chromogram of Bands of Frequency. *Measurement*, 135, 71–82.

DOI: [10.1016/j.measurement.2018.11.029](https://doi.org/10.1016/j.measurement.2018.11.029)

© 2018 Elsevier Ltd. All rights reserved.



This work is licensed under a [Creative Commons Attribution-NonCommercial-NoDerivatives 4.0 International License](https://creativecommons.org/licenses/by-nc-nd/4.0/).

# Condition monitoring of critical mechanical elements through Graphical Representation of State Configurations and Chromogram of Bands of Frequency

Alejandro Bustos\*, Higinio Rubio, Cristina Castejon, Juan Carlos Garcia-Prada

MAQLAB Research group, Department of Mechanical Engineering, Universidad Carlos III de Madrid, Av. de la Universidad, 30, 28911 Leganes (Madrid), Spain;  
albustos@ing.uc3m.es (A.B.); hrubio@ing.uc3m.es (H.R.); castejon@ing.uc3m.es (C.C.);  
jcgrada@ing.uc3m.es (J.C.G.P.)

\*Correspondence: albustos@ing.uc3m.es; Tel.: +34-91 624-8329

## Abstract

Fault detection is a crucial aspect to avoid catastrophic failures on mechanical systems, as well as to save money for companies. Currently, a number of non-destructing tests, signal processing analysis and artificial intelligence techniques are used for processing larger and larger amounts of maintenance data in all industry fields, either independently or combined. This manuscript presents a novel methodology for the condition monitoring of machinery, based on vibration analysis. The methodology is supported on two novel signal processing techniques: Graphical Representation of State Configurations (GRSC) and Chromogram of Bands of Frequency (CBF). These two new techniques apply basic concepts of the machine deterioration theory to the frequency spectrum. In order to prove the successful of the work presented, the methodology is tested against two real examples: vibration signals from the Case Western Reserve University (CWRU) Bearing Data Centre, and vibration signals from a high-speed train in normal operation. The results show that these new techniques can process large amounts of data without using artificial intelligence, identify adequately the operating condition of the tested systems and give precise information about that operating system by means of simple graphs and colours.

## Keywords

GRSC, CBF, condition monitoring, signal processing, rolling bearing, high speed train

## 1. Introduction

The application of condition monitoring to machines is a key aspect to get a good maintenance strategy that allows cost reductions in the current competitive markets. However, it requires reliable condition monitoring techniques and the ability to process an increasingly amount of data. Vibration analysis has advantages over other methods (like oil analysis, thermography, etc.) because it reacts immediately to changes, allows permanent and intermittent monitoring and, most important, a lot of signal processing techniques can be applied to vibration signals [1].

In this regard, Lee et al. review the most common used methods and algorithms applied to the diagnosis of rotatory mechanical systems in reference [2]. The two most classical methods for diagnosis are the time domain analysis and the Fourier transform. However, the application of these methods may not be sufficient to establish the condition

of the monitored system (especially with the current industrial requirements for mechanical elements that increasingly work in more critical conditions). As result of that, several techniques were developed to analyse the state of the system in the time-frequency domain, from a statistical point of view or using artificial intelligence methods.

Within the time-frequency domain, techniques like the Short-Time Fourier Transform [3], the Wavelet Transform [4] and the Hilbert-Huang Transform [5] are widely used for the condition monitoring of mechanical systems. Lots of works in the scientific literature apply these techniques to the identification of bearing defects [6–8]. However, these methods are also successfully applied to the analysis of transient vibration signals [9]; as well the condition monitoring and the identification of defects in complex mechanical systems like laboratory test benches [10,11] and real systems like rail vehicles [12,13].

Over the years, several techniques based on statistical concepts arisen and are employed in the monitoring of mechanical systems now. Among these methods, we can highlight the Principal Component Analysis (PCA) [14], the Statistical Pattern Recognition (SPR) [15] and the Kalman filters [16]. The PCA is applied to analyse the degradation of bearings [17] and gears [18]. Several works of the literature apply the SPR for the monitoring of various mechanical elements in different engineering fields [19–21]. Lastly, the application of Kalman filters has proved to be a useful tool for the isolation of specific features that allow to identify faults in such different complex machines like rail vehicles [22] and direct-drive wind turbines [23].

Frequently, the previous techniques (and other similar approaches) are combined with artificial intelligence methods like the Artificial Neural Networks [24], the Support Vector Machines [25] or the Fuzzy Logic [26]. That way, the advantages of the classical techniques are enhanced, so large amounts of data can be handle and thus obtain better results in the identification of defects in mechanical elements or systems [6,10,11,17,27,28].

Most of the works of the scientific literature apply the previous techniques to study a specific mechanical element. In this paper, the authors present a new methodology for monitoring the evolution of complex mechanical systems (made up of tens or hundreds mechanical elements) and detect performance changes due to faults, maintenance actions or other significant event. This methodology is based on the multi-level analysis and the development of two new signal processing techniques called Graphical Representation of State Configurations (GRSC) and Chromogram of Bands of Frequency (CBF). These new techniques combine some aspects of the methods described previously.

The structure of the paper is as follows. The second section depicts the basic concepts for the methodology development briefly and also describes the proposed methodology and the mathematical methods. The third section presents the experimental validation through two examples and discuss obtained from the application of the new techniques. The last section states the conclusions.

## **2. Methodology**

This section presents the theoretical concepts on which the designed methodology is supported and then, the methodology and proposed techniques for the processing of vibration signals are described.

### **2.1. Theoretical concepts**

The methodology presented in this manuscript is based on the time evolution of the vibration level of a machine or mechanical system. According to references [29,30], three

periods can be distinguished in the life of a machine. The first period corresponds to the running-in of the machine, in which young failures may occur. During this stage, the overall vibration level of the machine decreases. The second period is the normal operation of the machine, in which the vibration level increases very slowly due to the normal wear. The last period corresponds to a rapid increase of the vibration level as the machine approaches to breakdown. The graphical representation of this evolution is commonly known as the ‘bathtub’ curve.

At the third stage, a maintenance action or a repair will be needed to keep the machine in service. This event improves the condition of the machine and returns the state of the machine to the first period.

The methodology applies these concepts to the frequency domain and develops mathematical methods to represent the power time evolution of different frequency bands.

## **2.2. Methodology flowchart**

The flowchart of the proposed methodology is summarized in Figure 1 and has two starting points concerning to the mechanical system definition and the measurement conditions. The first starting point is the definition of the system to monitor. This step encompasses the classification of the machine type and the characterization of the relevant mechanical system or sub-system. The other starting point is the definition of the measurement conditions. Here there are two options: if laboratory tests are conducted, then the speeds, loads and defects on the machine are set as required. However, if the system operates in normal condition (real system), the measurement conditions must be stated according to the availability of the machine.

The design of the measurement system takes into account the inputs from the system definition and the measurement conditions. The number, type, characteristics and position of the sensors must be established at this step; as well as the data acquisition software.

The vibration measurements are recorded in a dedicated database. Later, the recorded data are extracted, grouped according to the measurement conditions and processed in the time, frequency and/or time-frequency domains. In this paper, we will only focus on the frequency domain, as it is the basis of the new proposed methods. First, the PSD of the signals is computed and, then the average spectra and spectral power of each signal groups is obtained.

Next, the MLA (Multi-Level Analysis), GRSC and CBF techniques are applied and the results are analysed.

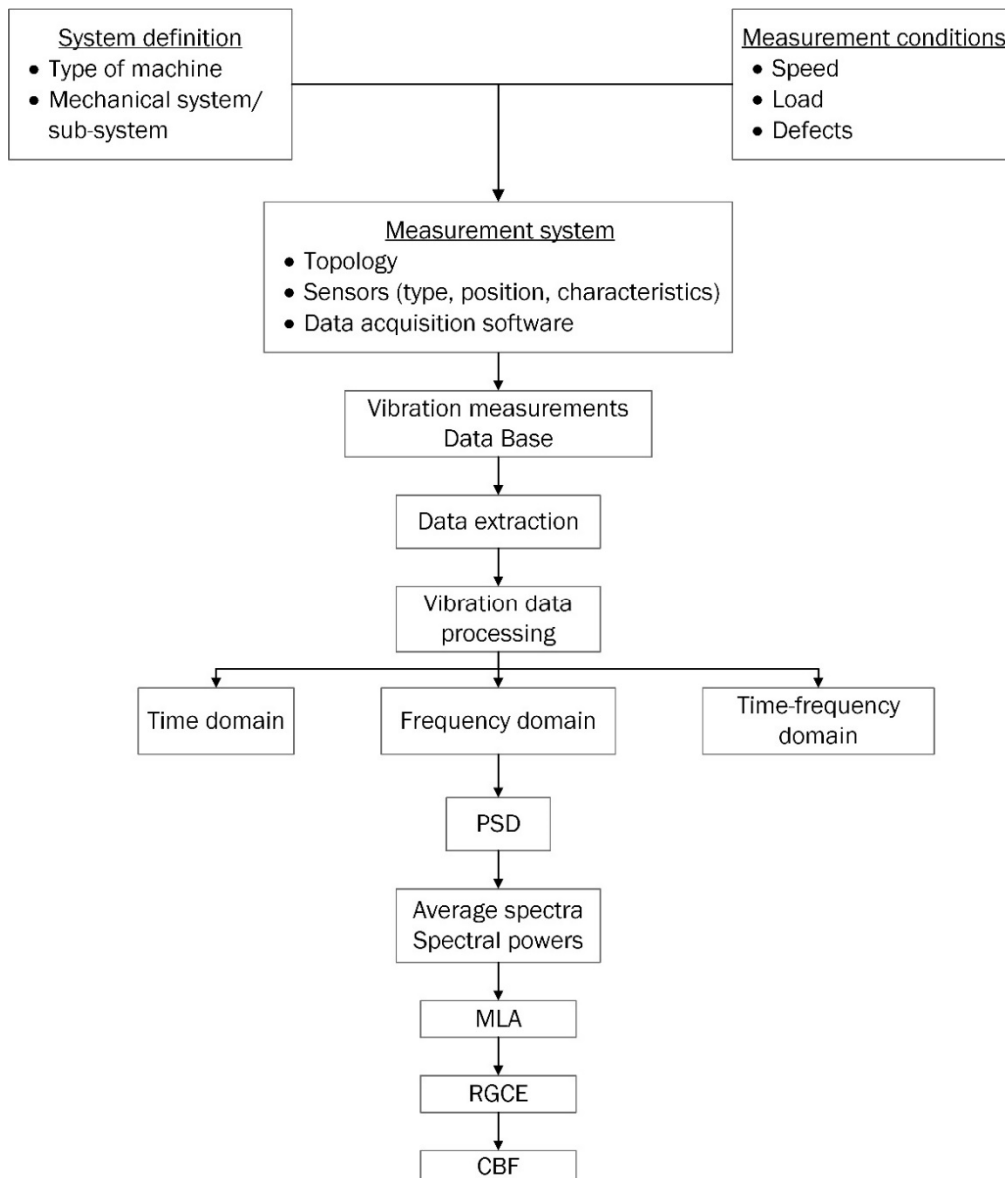


Figure 1. Scheme of the proposed methodology.

### 2.3. Multi-Level Analysis (MLA)

The first step in order to obtain the CBF is the decomposition of the frequency spectrum in several frequency bands or power packets. This task is made by applying the Multi-Level Analysis (MLA). This method divides the frequency spectrum in  $2^k$  bands, with  $k$  the decomposition level. Each frequency band is associated to a part of the total spectral power. The Figure 2 shows the decomposition procedure starting from the PSD of a signal.

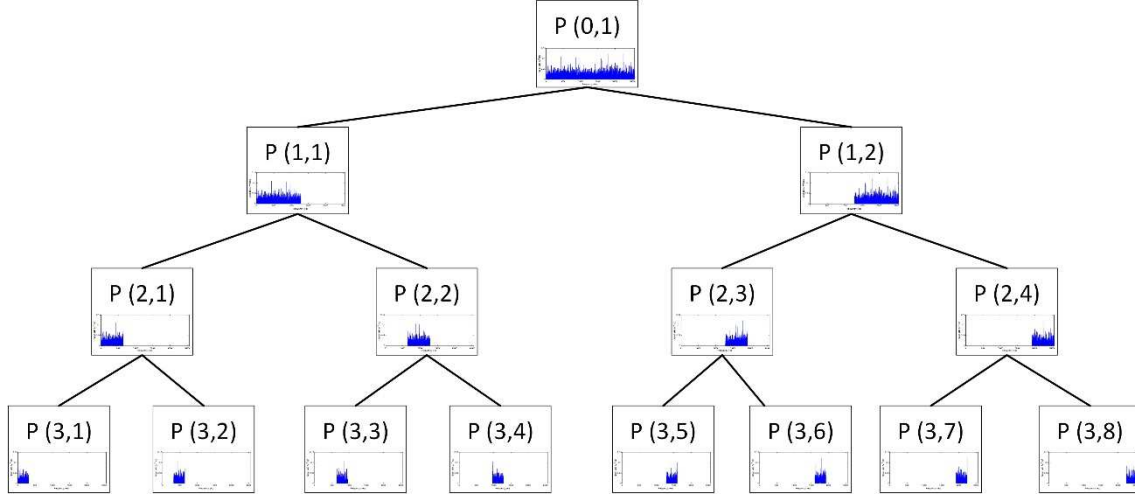


Figure 2. Scheme of the decomposition process (MLA).

The Equation (1) defines the decomposition algorithm for a decomposition level  $k$  of a PSD. The value of  $k$  must be such that the result  $2^k$  will be always less or equal to the number of points  $N$  in the vibration signal, that is to say,  $2^k \leq N$ , and results an integer.

$$P(k, j) = \sum_{j=1}^{j=2^k} \sum_{i=\frac{N}{2^k}(j-1)+1}^{i=\frac{N}{2^k}j} S_x(i) \quad (1)$$

Where  $i$  is the index of the signal's vector,  $j$  is the packet's number for a decomposition level  $k$ ,  $k$  is the decomposition level,  $N$  is the number of points of the signal,  $S_x(i)$  is the value of the PSD at index  $i$ , and  $P(k, j)$  is the power of the packet  $j$  for the decomposition level  $k$ .

The algorithm can also be applied not only to the PSD, but also the spectrum of the envelope of the signal. So the equation (1) can be rewritten as equation (2):

$$P_H(k, j) = \sum_{j=1}^{j=2^k} \sum_{i=\frac{N}{2^k}(j-1)+1}^{i=\frac{N}{2^k}j} S_H(i) \quad (2)$$

Where all the parameters represent the same as equation (1) except  $S_H(i)$ , which is the value of the spectrum of the Hilbert transform at index  $i$ , and  $P_H(k, j)$ , which is the power of the packet  $(k, j)$  of the envelope spectrum.

Obviously, the bandwidth of the resulting packets varies with the decomposition level. The higher the decomposition level, the smaller the bandwidth. The Table 1 shows the relation between the bandwidth and the decomposition level  $k$  (up to level  $k=9$ ), taking as example a Nyquist frequency of 2560 Hz.

Table 1. Bandwidth for different decomposition levels, taking a Nyquist frequency of 2560 Hz.

<b>k</b>	<b>0</b>	<b>1</b>	<b>2</b>	<b>3</b>	<b>4</b>	<b>5</b>	<b>6</b>	<b>7</b>	<b>8</b>	<b>9</b>
<b><math>2^k</math></b>	1	2	4	8	16	32	64	128	256	512
<b>Bandwidth <math>f_{\text{Nyquist}}/2^k</math> (Hz)</b>	2560	1280	640	320	160	80	40	20	10	5

## 2.4. Definition of the operating states

Before the application of the new methods, three operating states must be defined. These operating states are established taking as reference a significant event or change in the mechanical system, i.e. a maintenance operation. The first operating state, called B (Before), groups all the measurements recorded before the significant event. The second operating state, named A (After), collects the measurements taken just after the significant event. The third and last operating state is called L (Later). This operating state groups all the measurements recorded after a period of time since the significant event.

## 2.5. GRSC

The GRSC (Graphical Representation of State Configurations) is a graphical representation for the time evolution of the power of each packet. This evolution is displayed as a triangle whose vertices are the value of the average power of the packets of each operating state.

The process to build the GRSC is shown in Figure 3 and works as follows:

Let be a data set with  $n$  vibration signals which have been decomposed in  $m$  power packets  $P(k,j)$ . The  $n$  power packets, corresponding to a decomposition level  $k$  ( $n=2^k$ ) and a decomposition index  $j$ , are grouped in the three operating states defined above. Then, the average power and date of each operating state are computed, and three points (B, A, L) with coordinates time and power are obtained.

Next, the significant event is marked in the time axis (step 1 of Figure 3) and the three points are plotted in the time-average power axes (steps 2-4 of Figure 3). Later, these points are joined with straight lines.

The straight line joining the operating states B and A is always plotted in red (step 5 of Figure 3). The operating states A and L are linked using a green line (step 6 of Figure 3), and the states B and L are connected with a blue line (step 7 of Figure 3).

In addition, a coding for the easy identification of the configuration of the operating states has been defined (step 8 of Figure 3). This coding consists of three colours (red, green and blue) and three letters (B, A, L) naming each of the three lines in the same order that are generated. These letters are written in uppercase or lowercase letters according the sign of the slope of the straight line joining two operating states. Uppercase letters correspond to slopes greater or equal to zero, while lowercase letters correspond to negative slopes.

That way, taking as example a bAl configuration, that means the power of packet  $P(k,j)$  is reduced between states B and A, and between states B and L; however the power is increased between states A and L. In principle, the bAl or bal are the expected configurations in the analysis of a mechanical system which have been repaired recently (from the third period of the 'bathtub' curve to the first period). In case the apparition of a defect will be studied, the expected configurations would be BAL or BaL (from the second period of the 'bathtub' curve to the third period). The Table 2 shows all the configuration possibilities accompanied by an explanatory drawing and the previous colour coding.

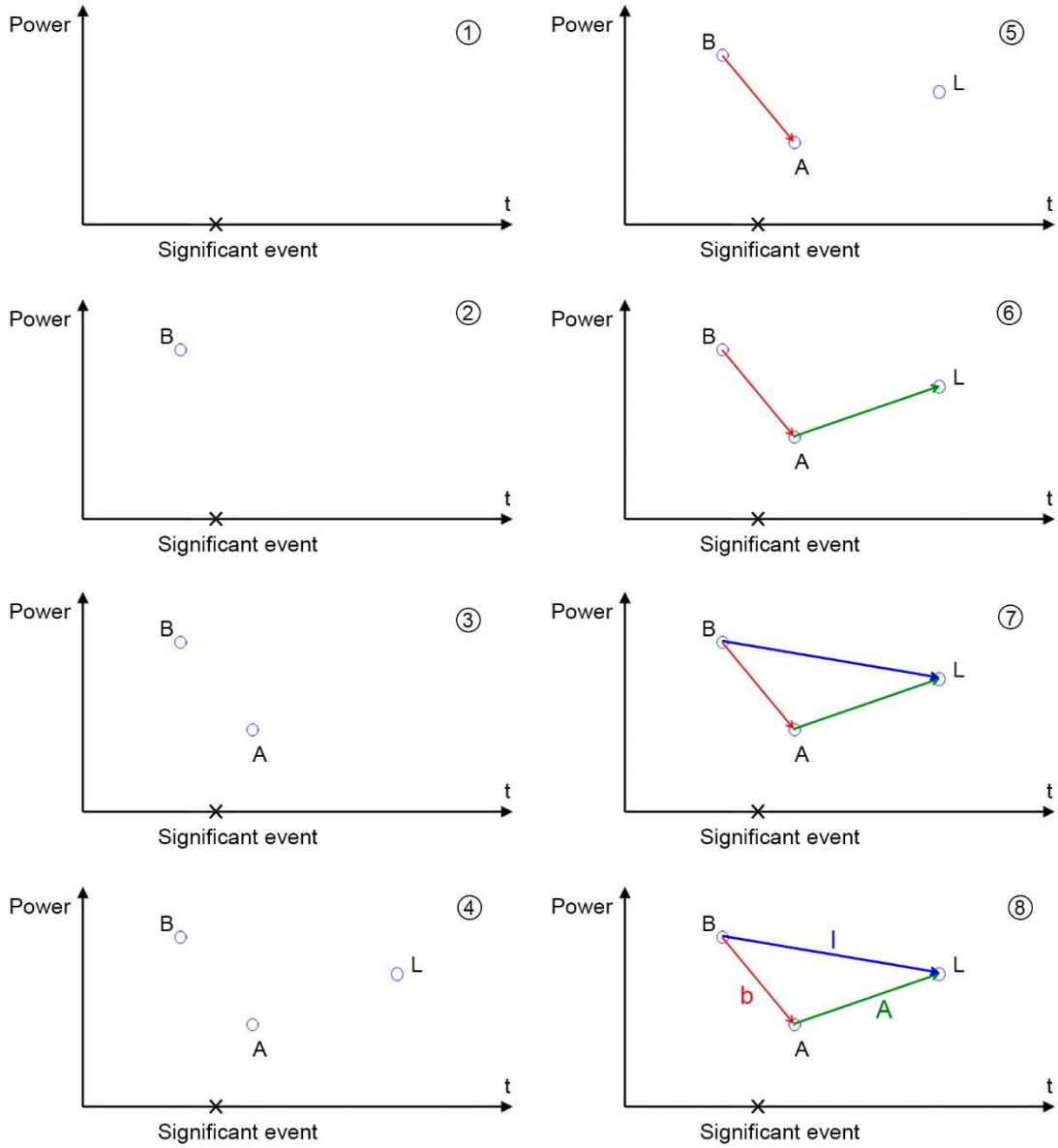


Figure 3. Generation process of GRSC.



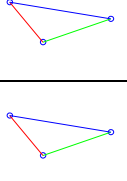
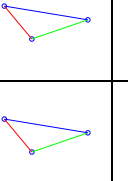
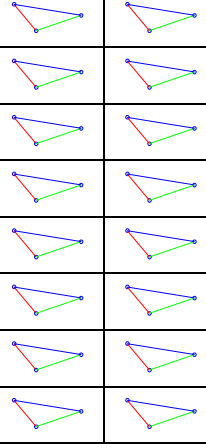
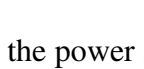
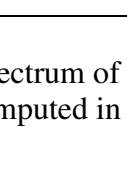
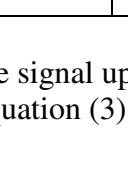

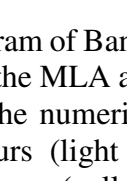
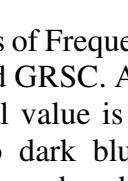
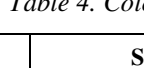
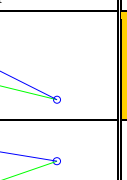
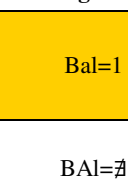
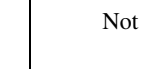


Table 2. Possible configurations

Configuration	Shape	Configuration	Shape
$baL=-3$		$BaL=1$	
$bAl=-2$		$BAL=\neq$	Not possible
$baL=\neq$	Not possible	$BaL=2$	
$bAL=-1$		$BAL=3$	



The number of configuration of states shapes is directly related to the decomposition level of the signal's spectrum. As the spectrum is split in two halves each time,  $2^k$  shapes are obtained per  $k$  level. The Table 3 shows this phenomenon.

Table 3. Increase of shape number with decomposition level

k	0	1	2	3	4	...
Shapes						...
						
						
						
						

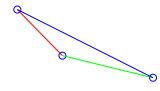
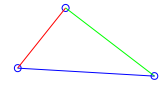
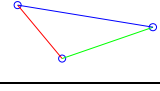
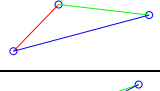
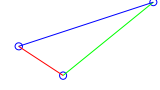
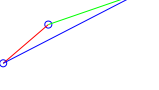
If we decompose the power spectrum of the signal up to, for example, level  $k=9$ , we will obtain 1023 shapes, as it is computed in equation (3).

$$\text{Number of triangles} = \sum_{k=0}^9 2^k = 2^{(sup k+1)} - 1 = 2^{9+1} - 1 = 1023 \quad (3)$$

## 2.6. CBF

The aim of the CBF (Chromogram of Bands of Frequency) is to compile in one image all the information extracted from the MLA and GRSC. A numerical value is assigned to each GRSC configuration. Then the numerical value is converted in a specific colour according to Table 4, cold colours (light to dark blue) corresponds to negative b configurations, while warm colours (yellow and reds) corresponds to positive B configurations.

Table 4. Colour coding of the possible configurations

Configuration	Shape	Configuration	Shape
baL=-3		BaL=1	
bAL=-2		BAL=∅	Not possible
baL=∅	Not possible	BaL=2	
bAL=-1		BAL=3	

Then the energy packets are plotted in a colour map according to their frequency, bandwidth, decomposition level and colour. The Figure 4 shows an example of a CBF. For a better understanding of the CBF technique, the configurations of decomposition level  $k=2$  have been marked in the figure.

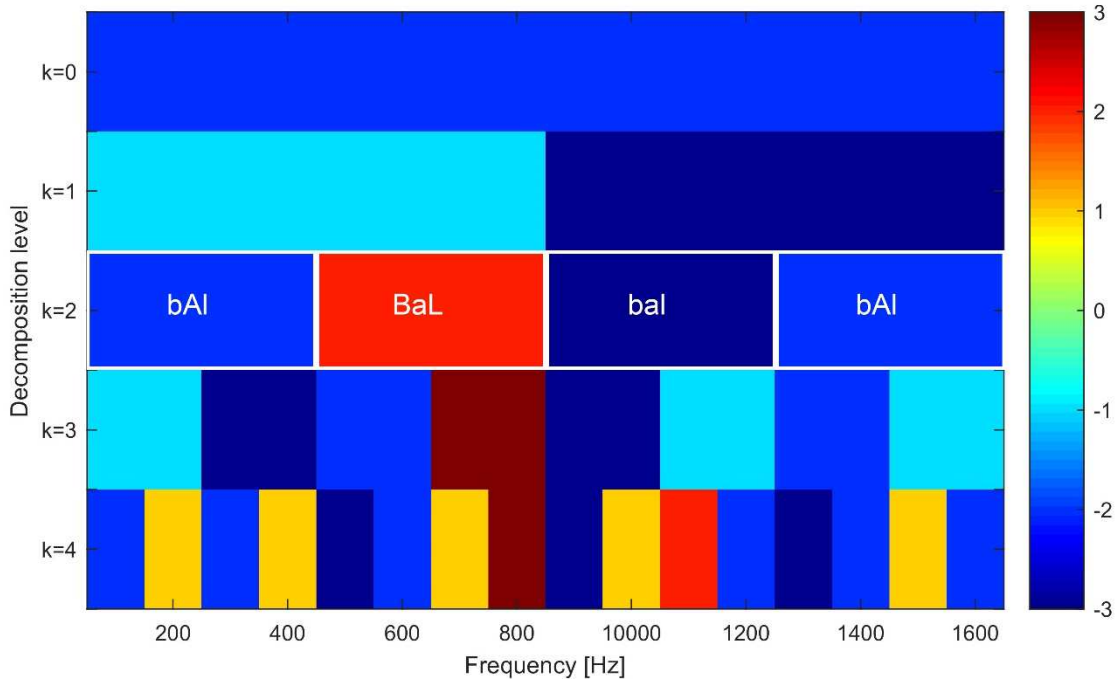


Figure 4. Example of CBF

The presented techniques are especially developed for monitoring complex mechanical systems and the identification of performance changes in those system due to events like maintenance operation or the apparition of defects in one of the mechanical elements of the system, among others.

The GRSC is a good method to oversee the trends in the evolution of the mechanical system, while the CBF can offer a global view of the system and highlight the critical frequency bands. So they can be used jointly or separately, according to the objectives of the monitoring.

### 3. Experimental validation

This section presents the experimental validation of the proposed techniques and methodology through two examples. The first example uses a well-known vibration database of bearing faults and the second one considers real signals taken from a high speed train (HST) during its normal operation. The subsections of both examples describe the experiments in first place and then discuss the obtained results.

#### 3.1. Bearing data

Ball bearing test data from the Case Western Reserve University Bearing Data Centre [31] were used for the first experimental validation. These data have been widely used in the scientific literature and it is a de facto standard for testing new methods for detecting bearing defects. In reference [32], Smith and Randall conduct a benchmark over those data and provide very useful information about the signals.

### 3.1.1. Description of the experiment

The test bench consist of a 2 horsepower motor, a torque transducer/encoder and a dynamometer. The tested bearings support the motor shaft. Vibration data were collected using accelerometers located at the drive and fan ends of the motor and with a sampling rate of 48000 samples per second. The Figure 5 shows the test rig used at CWRU for testing bearings.

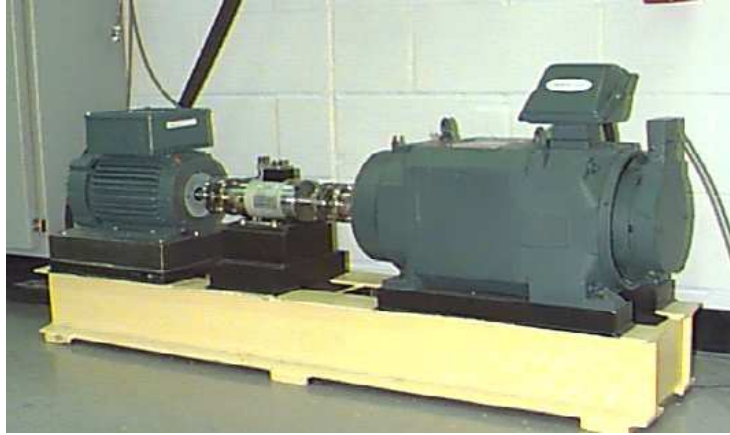


Figure 5. Test rig of the CWRU Bearing Data Centre [31]

Of all the available data in the repository, we will focus on the ball faults data. Three different states were downloaded (fault diameters of 7 and 14 mils of inch, and without faults). These data are arranged to simulate the usual trend of a faulty machine after the appearing of a defect. So, the definition of the operating states is as follows:

- State B (Before) corresponds to the baseline (no defects) signal.
- State A (After) corresponds to the 7 mils defect signal
- State L (Later) corresponds to the 14 mils defect signal.

The Figure 6 shows the appearance of the vibration signals without defect and with 7 mils defect, as well as their spectra.

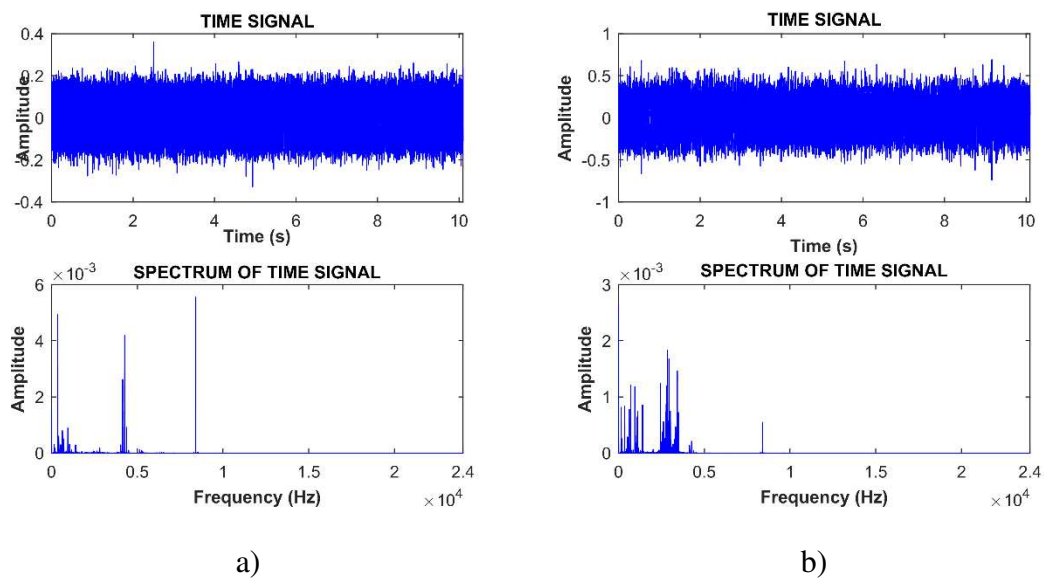


Figure 6. Time signal and spectrum of CWRU signals: a) normal baseline and b) ball 7mils defect.

### 3.1.2. Results and discussions

Due to the fact that the bearing measurements have different lengths, they were split in sections of 16384 data points, resulting in 29 subsignals from each original signal. Then, the proposed methodology is applied to the bearing signals and the spectra are broken down into packets up to level  $k=11$ . The results of applying the GRSC to the drive end (DE) vibration signals are shown in Figure 7.

For a decomposition level of  $k=0$  the shape of the state configuration is the expected: a power increase after the apparition of the defect that grows as the defect size becomes bigger and bigger. This behaviour corresponds to a BAL configuration.

The two power packets of the decomposition level  $k=1$  show different shapes. The power packet between 0 and 12 kHz presents the expected BAL configuration; whereas the power packet between 12 and 24 kHz presents a bAl configuration, which indicates a power reduction from state B to state A and a power increase between state A and state L with a power reduction between state B and state L.

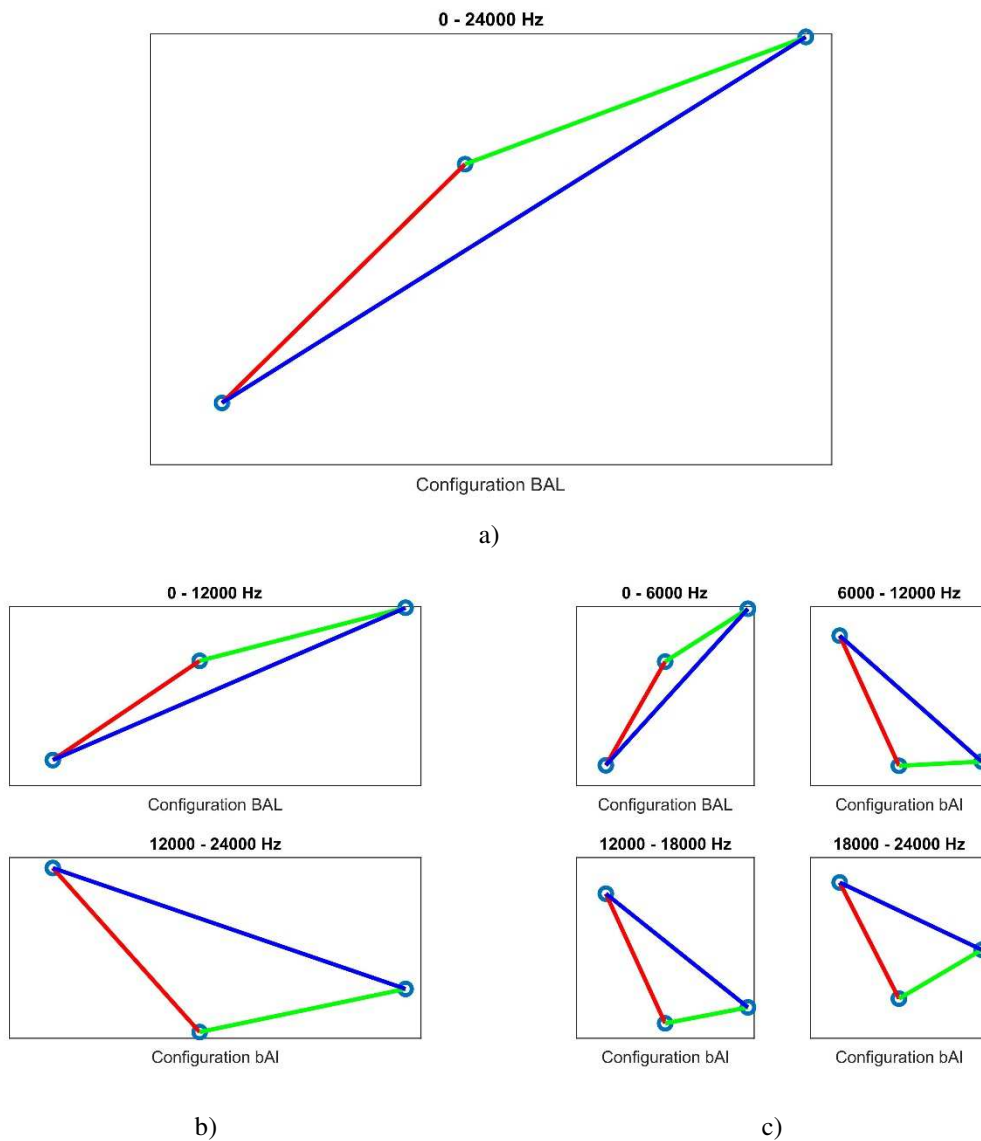


Figure 7. GRSC of the DE vibration signals for decomposition levels  $k=0$  (a),  $k=1$  (b) and  $k=2$  (c).

For a decomposition level  $k=2$ , we obtain four power packets in the frequency bands 0-6 kHz, 6-12 kHz, 12-18 kHz and 18-24 kHz. The first one (0-6 kHz) shows a BAL

configuration as expected. However, the other three power packets present a bAI configuration.

According to the states definition made in section 2.5 –which are based on the time degradation curve explained in section 2.1 – the obtained shapes indicate the presence of a defect and also that this defect is more perceptible in the low frequency range.

The CBF is shown in Figure 8. First, we can check that the colours of the horizontal strips  $k=0-2$  matches the configurations stated in Table 4. Red colours —especially dark-red— are the dominant colours below 4000 Hz in all the decomposition levels. The large frequency band between 4000 Hz and 21600 Hz is dominated by blue colours, with some small stripes of yellow and red. The frequency band between 21.6 kHz and 24 kHz presents a red strip.

A detailed view of the 0-3000 Hz frequency band is shown in Figure 9. In this detail, we can see a significant zone coloured in light blue, which means a reduction of the vibration level between the state B (no defect) and the state A (7 mils defect). However, between the states B and L, the power is increased. This phenomenon could be originated by the measuring issues detected by Smith and Randall in reference [32]. The red colours in the frequency bands that contain the BSF and 2xBSF indicate a vibration level increase in that bands, which confirms this method can detect the ball fault and improves the results of the three methods proposed in [32].

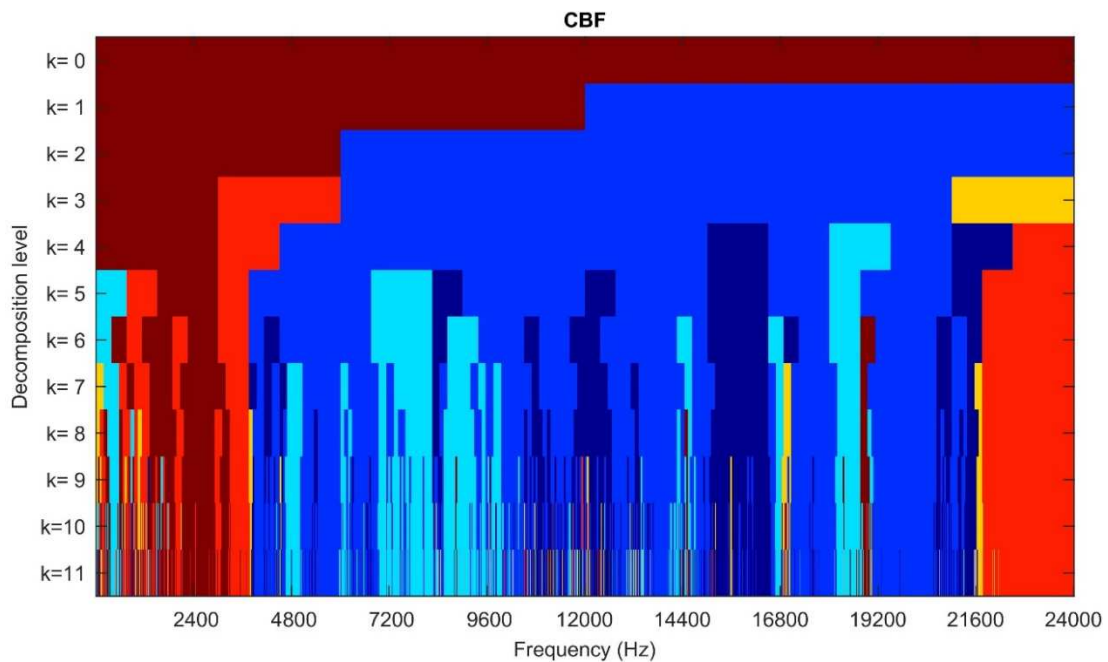


Figure 8. CBF of the DE vibration signals.

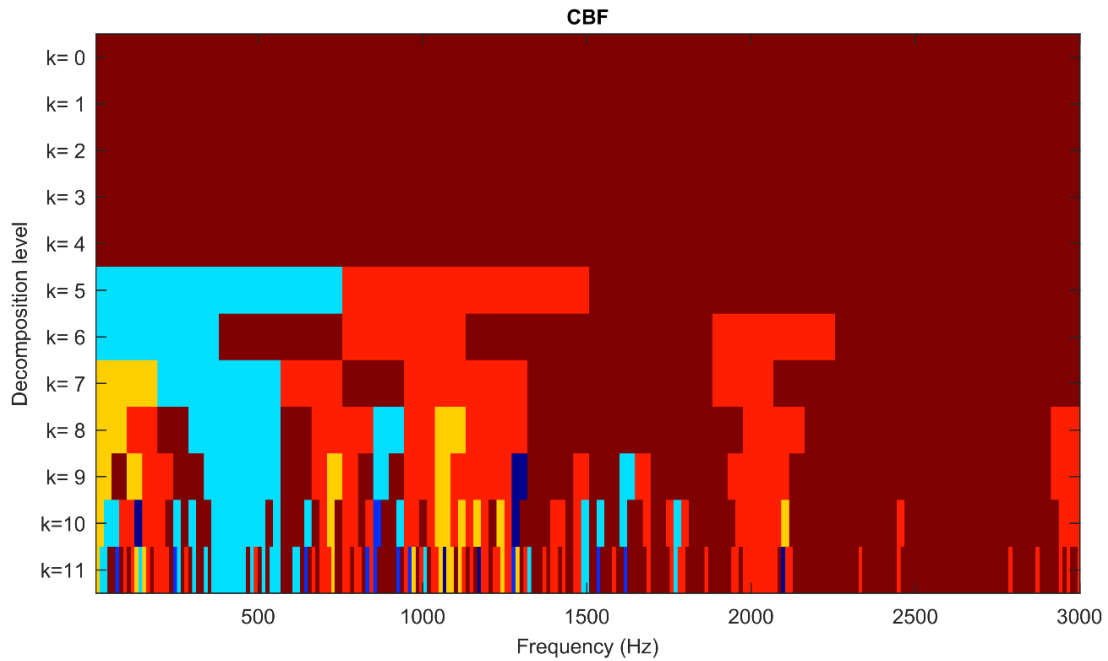


Figure 9. Detail of the CBF of the DE vibration signals in the 0-3000 Hz frequency band.

### 3.2. HST axle box vibrations

The second experimental validation of the proposed methods is carried up with vibration data from a high speed train. The train under study is equipped with a vibration measuring system (composed of several accelerometers), a data acquisition system, and a communication system that transmits the data to the cloud (see Figure 10). Then these data are downloaded and processed in a computer.

The accelerometers are placed in the axle box cover of a trailer axle. This axle is part of the last bogie of the last passenger car and is the nearest axle to the second power car. In this paper, we will only focus on the vertical accelerometer – highlighted in yellow in Figure 10.

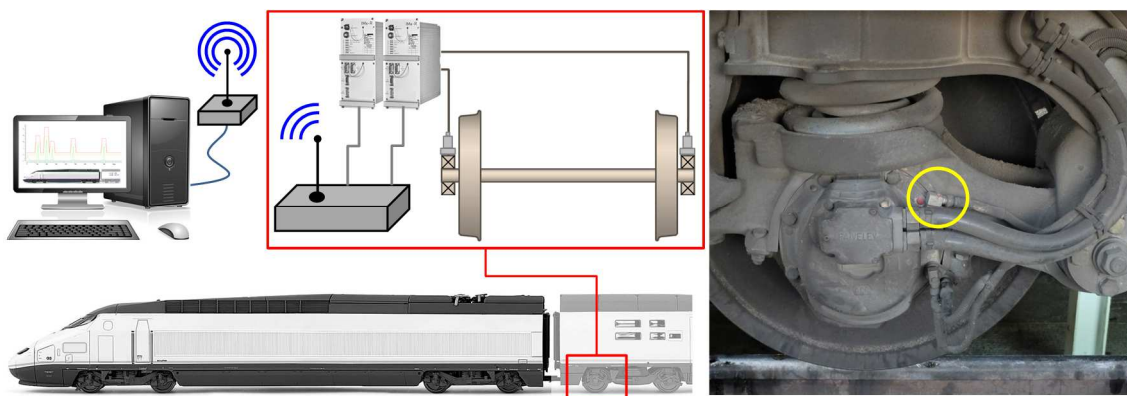


Figure 10. Diagram of the measurement system and location of the vertical accelerometer.

#### 3.2.1. Description of the experiment

Vibration data were collected from a high speed train during its normal operation. Accelerometers were placed in the axle box and measurements were taken at an average speed of 270 km/h in a selected section of a Spanish high speed line. The vibration signals

were acquired at a sampling rate of 5120 Hz. Full details of the measurement system and conditions can be found in [33].

The train underwent a maintenance operation that consisted of the reprofiling the two wheels of the monitored axle. The vibration signals are analysed before and after the maintenance works. The Figure 11 shows two examples of vibration signals before and after the maintenance, as well as their spectra. Taking into account the maintenance date, three different operating states are defined:

- State B (Before): it groups all the vibration data collected before the maintenance action. The average power of this state is depicted by the B points in Figure 12.
- State A (After): it groups all the vibration data collected just after the maintenance action. In this case, the first day after returning to service. The average power of this state is represented by the point located in the middle of the images of Figure 12.
- State L (Later): it groups all the vibration data recorded after the state A. The average power of this state is illustrated by the most right point in the graphs of Figure 12.

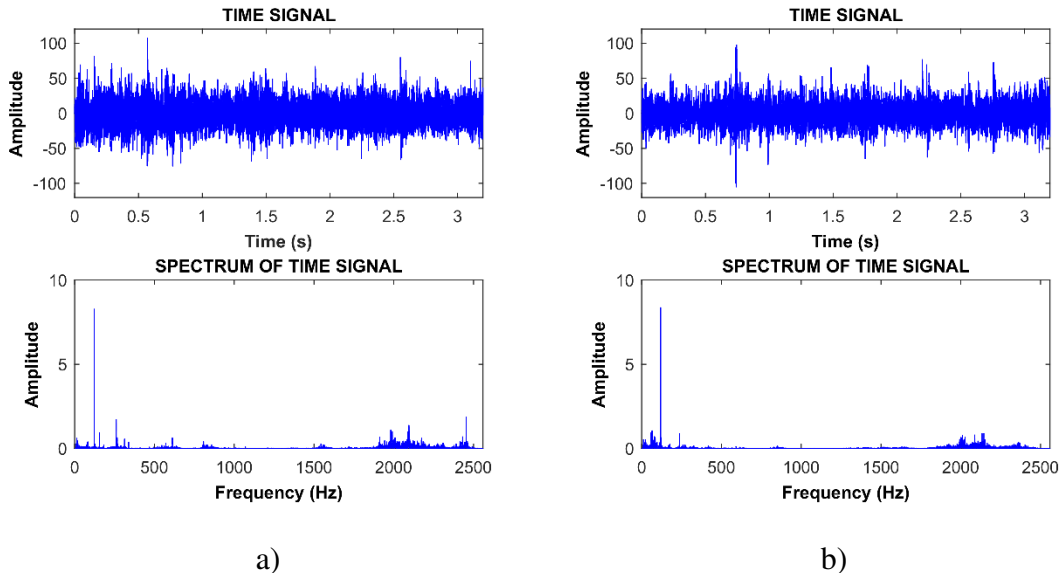


Figure 11. Time signal and spectrum of the HST vibration signals before (a) and after (b) the wheel intervention.

### 3.2.2. Results and discussions

In this experiment, 1234 signals are processed following the proposed methods. First, the PSD of each recorded signal is computed and averaged. Then the average spectra of the three operating states are split in power packets from decomposition level  $k=0$ , namely the whole spectrum, up to decomposition level  $k=9$ .

The Figure 12 shows the GRSC of the decomposition levels  $k=0-3$ . In the GRSC of level  $k=0$  –that is, the whole spectrum– it is clearly visible a spectral power reduction between the states B and A. This means that the maintenance operation has reduced the vibration level of the system. If we focus on the evolution between states A and L, we observe an increase of the spectral power, which is consistent with a gradual deterioration of the system after the overhaul. The negative slope between states B and L means the spectral power has not reached the level previous to maintenance yet.

The two power packets of the decomposition level  $k=1$  (see Figure 12 b) present different configurations. The low frequency packet shows a bAL, which means an increase of the vibration level at the end of the studied process. On the other hand, the bal configuration of the high frequency packet means a continuous descent of the vibration level.

The decomposition level  $k=2$  gives four state configurations (Figure 12 c). The power packets 1 (0-640 Hz) and 3 (1280-1920 Hz) present the bAl configuration; while the fourth power packet (1920-2560 Hz) shows a bal configuration. The second power packet (640-1280 Hz) presents a BAL configuration, which –in this case– is the worst possible configuration, as the vibration level always raises.

The eight configurations of the decomposition level  $k=3$  are plotted in Figure 12 d. In this case, there is a great diversity of configurations. The first (0-320 Hz) and seventh (1920-2240 Hz) power packets present bal configurations. The power packets 5, 6 and 8 display a bAl configuration, while the second power packet exhibits a bAL configuration. The two remaining power packets (640-960 Hz and 960-1280 Hz) reveal a BAL configuration.

The Figure 13 shows the CBF of the PSD of the vertical vibrations, compiling the information of the 1023 configurations obtained from the decomposition process up to level  $k=9$ . The analysis of the CBF shows a predominance of blue colours over red colours, which means the vibration level is reduced after the maintenance action. The red zone is visible from decomposition level  $k=2$  and is mainly located in a frequency band between 800 and 1500 Hz.

There are also several zones where the power level is reduced after the wheels reprofiling operation in all the decomposition levels. That is, blue colours from the top to the down of the CBF. These frequency bands are located, approximately, at 400-750 Hz, 1500-1675 Hz and above 2000 Hz. However, they exist some zones within these bands that increase the power after the maintenance in the highest decomposition levels.

In short, the frequency bands of 400-750 Hz, 1500-1675 Hz and 2000-2500 Hz are affected positively by the maintenance action, while the frequency band between 800 and 1500 Hz suffers the opposite effect.

These results agree with the results presented in [12] using the EMD technique. However, the methods presented in this paper allow a faster and more visual identification of the critical zones of the frequency spectrum. In addition, these new techniques compile a lot of information in few images that would need lots of figures by using the methods applied in reference [12].



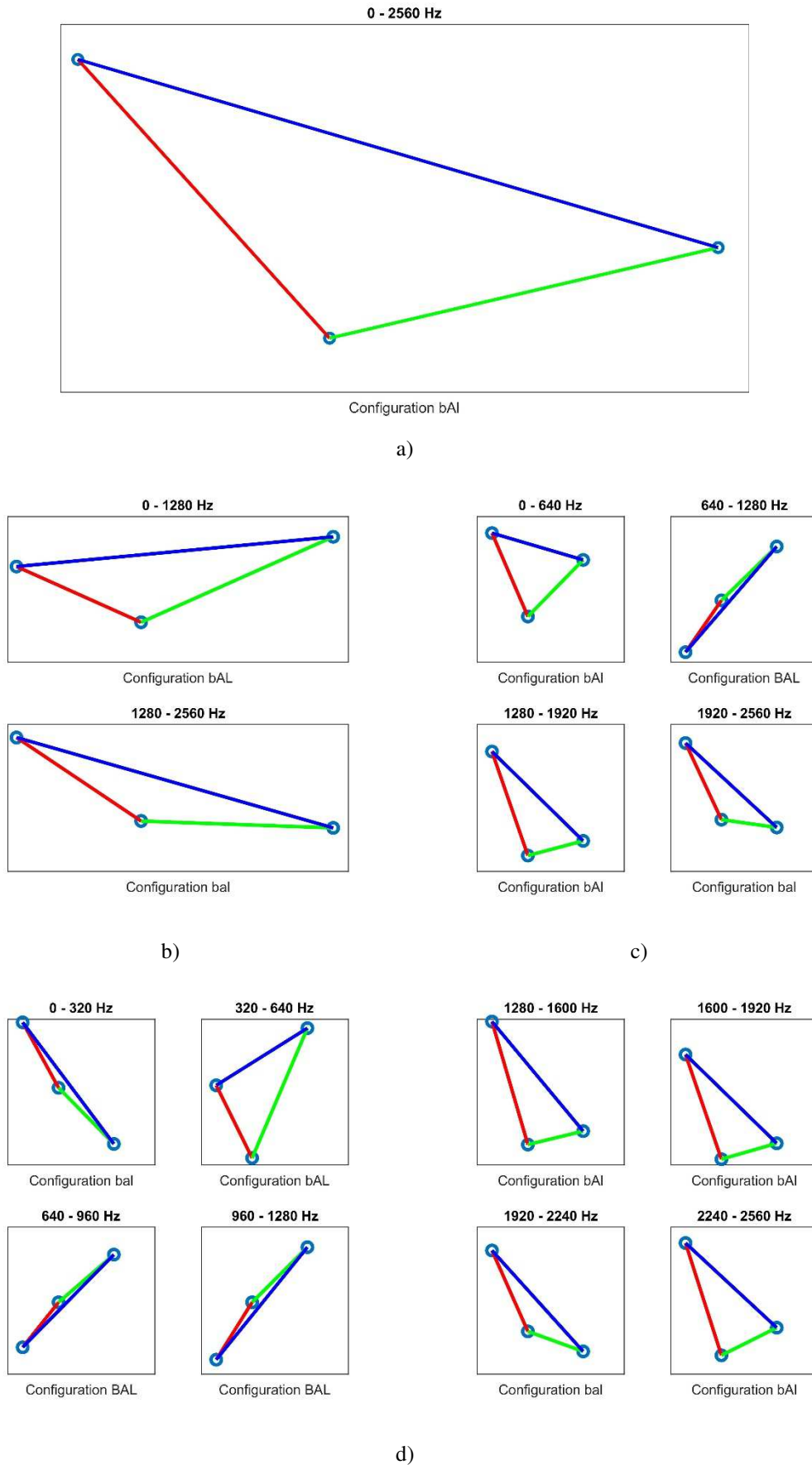


Figure 12. GRSC of the HST vibration signals for decomposition levels  $k=0$  (a),  $k=1$  (b),  $k=2$  (c) and  $k=3$  (d).

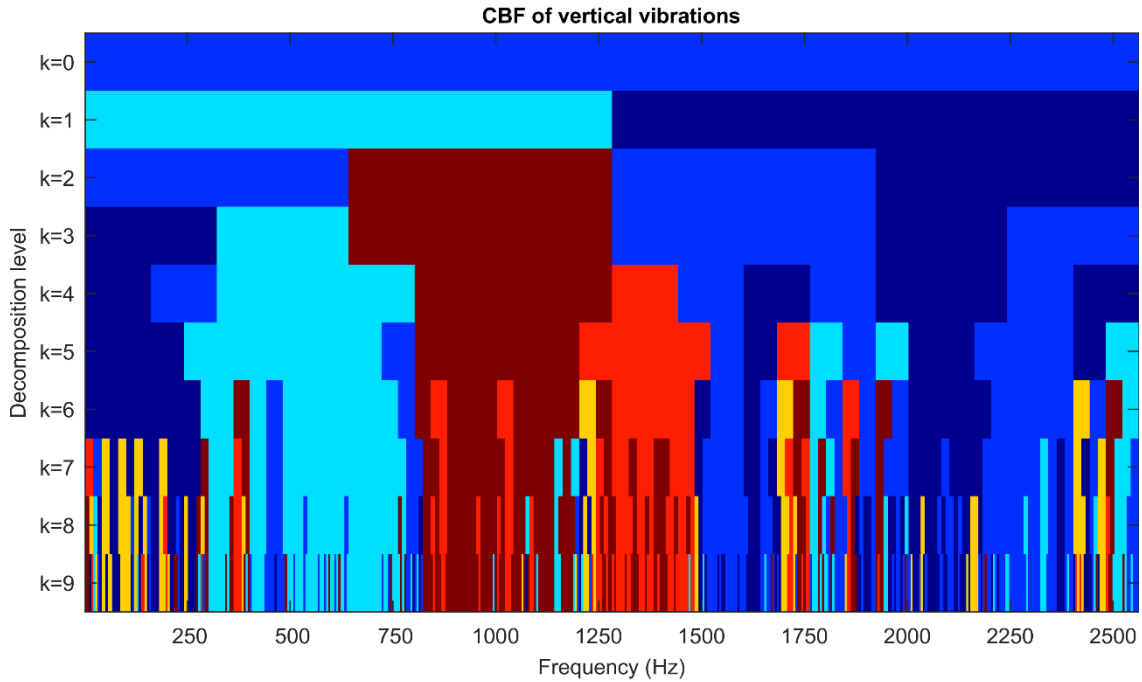


Figure 13. CBF of the vertical vibrations

#### 4. Conclusions

In this paper, a new methodology for the analysis of vibratory mechanical systems is proposed. The methodology uses two different novel techniques to represent, in a simple way, the large amount of vibration measurements that can be acquired when monitoring a complex mechanical system in order to evaluate its condition. The methodology is tested on a simple mechanical system such as a bearing test bench (evaluation of a single mechanical element through vibration measurements) and on a complex mechanical system such as the wheelset of a HST in operation.

The GRSC technique let classify the evolution of the power packets (from a PSD signal) in one of six possible configurations and synthesize the information in graphs.

The CBF technique let assign a unique colour to the possible GRSC configurations and compiles all the configurations obtained from the GRSC. Then these configurations are shown in the form of a colourmap with decomposition level-frequency axes.

The experimental validation has demonstrated the utility of the proposed techniques for the monitoring of simple and complex mechanical systems. The tests carried out have highlighted the advantages of the new methods over other classical techniques: the GRSC and the CBF can handle large amounts of data (without using artificial intelligence) and show the evolution of the machine condition in a simple way using graphs and colours. Basically, upward lines and red colours means the machine is working in worse conditions (greater vibration level), and downward lines and blue colours indicate the machine is running in better conditions (less vibration level). In addition, the GRSC and the CBF have been able to detect the presence of a defect that could not be identified in other works using classical methods. Lastly, the number coding of the CBF can be used as the input data of an intelligent system for continuous monitoring or further analysis.

The methodology is based on the existence of a milestone; however, this methodology can also be used on a daily monitoring by grouping the data recorded today in the L state, collecting the data recorded yesterday in the A state, and arranging all the data recorded before yesterday in the B state. Then, the user of the methodology must

only see the trend of the GRSC or the colours of the CBF to identify the condition of the monitored mechanical system.

## Acknowledgements

The research work described in this paper was supported by the Spanish Government through the MAQ-STATUS DPI2015-69325-C2-1-R project

## Conflict of interests

The authors declare no conflict of interest.

## References

- [1] R.B. Randall, *Vibration-based Condition Monitoring: Industrial, Aerospace and Automotive Applications*, John Wiley & Sons, Ltd, West Sussex, UK, 2010.
- [2] J. Lee, F. Wu, W. Zhao, M. Ghaffari, L. Liao, D. Siegel, Prognostics and health management design for rotary machinery systems—Reviews, methodology and applications, *Mech. Syst. Signal Process.* 42 (2014) 314–334. doi:10.1016/j.ymsp.2013.06.004.
- [3] J.B. Allen, Short term spectral analysis, synthesis, and modification by discrete Fourier transform, *IEEE Trans. Acoust. Speech Signal Process.* 25 (1977) 235–238. doi:10.1109/TASSP.1977.1162950.
- [4] I. Daubechies, ed., *Ten lectures on wavelets*, Society for Industrial and Applied Mathematics, 1992. doi:10.1137/1.9781611970104.
- [5] N.E. Huang, Z. Shen, S.R. Long, M.C. Wu, H.H. Shih, Q. Zheng, N.-C. Yen, C.C. Tung, H.H. Liu, The empirical mode decomposition and the Hilbert spectrum for nonlinear and non-stationary time series analysis, *Proc. R. Soc. Lond. Math. Phys. Eng. Sci.* 454 (1998) 903–995.
- [6] H. Liu, L. Li, J. Ma, Rolling Bearing Fault Diagnosis Based on STFT-Deep Learning and Sound Signals, *Shock Vib.* 2016 (2016) 1–12. doi:10.1155/2016/6127479.
- [7] S. Mohanty, K.K. Gupta, K.S. Raju, Hurst based vibro-acoustic feature extraction of bearing using EMD and VMD, *Measurement.* 117 (2018) 200–220. doi:10.1016/j.measurement.2017.12.012.
- [8] H. Cao, F. Fan, K. Zhou, Z. He, Wheel-bearing fault diagnosis of trains using empirical wavelet transform, *Measurement.* 82 (2016) 439–449. doi:10.1016/j.measurement.2016.01.023.
- [9] J.-Y. Lee, Variable short-time Fourier transform for vibration signals with transients, *J. Vib. Control.* 21 (2015) 1383–1397. doi:10.1177/1077546313499389.
- [10] Y. Han, B. Tang, L. Deng, Multi-level wavelet packet fusion in dynamic ensemble convolutional neural network for fault diagnosis, *Measurement.* 127 (2018) 246–255. doi:10.1016/j.measurement.2018.05.098.
- [11] M.J. Gómez, C. Castejón, J.C. García-Prada, Automatic condition monitoring system for crack detection in rotating machinery, *Reliab. Eng. Syst. Saf.* 152 (2016) 239–247. doi:10.1016/j.res.2016.03.013.
- [12] A. Bustos, H. Rubio, C. Castejón, J. García-Prada, EMD-Based Methodology for the Identification of a High-Speed Train Running in a Gear Operating State, *Sensors.* 18 (2018) 793. doi:10.3390/s18030793.
- [13] Z. Li, L. Wei, H. Dai, Y. Zeng, Y. Wang, Identification method of wheel flat based on Hilbert-Huang transform, *J. Traffic Transp. Eng.* 12 (2012).

- [14] I.T. Jolliffe, *Principal Component Analysis*, 2nd ed., Springer-Verlag New York, New York, USA, 2002.
- [15] A.R. Webb, *Statistical pattern recognition*, 2nd ed, Wiley, West Sussex, England ; New Jersey, 2002.
- [16] R.E. Kalman, A New Approach to Linear Filtering and Prediction Problems, *J. Basic Eng.* 82 (1960) 35–45. doi:10.1115/1.3662552.
- [17] S. Dong, T. Luo, Bearing degradation process prediction based on the PCA and optimized LS-SVM model, *Measurement*. 46 (2013) 3143–3152. doi:10.1016/j.measurement.2013.06.038.
- [18] C.Y. Yang, T.Y. Wu, Diagnostics of gear deterioration using EEMD approach and PCA process, *Measurement*. 61 (2015) 75–87. doi:10.1016/j.measurement.2014.10.026.
- [19] H. Sohn, C.R. Farrar, N.F. Hunter, K. Worden, Structural Health Monitoring Using Statistical Pattern Recognition Techniques, *J. Dyn. Syst. Meas. Control*. 123 (2001) 706. doi:10.1115/1.1410933.
- [20] D. Adams, J. White, M. Rumsey, C. Farrar, Structural health monitoring of wind turbines: method and application to a HAWT, *Wind Energy*. 14 (2011) 603–623. doi:10.1002/we.437.
- [21] A.A. Mosavi, K. Haverty, Application of a Statistical Pattern Recognition Technique for Integrity Monitoring of Umbilicals and Subsea Flowlines, in: *ASME*, 2015: p. V05BT04A043. doi:10.1115/OMAE2015-41010.
- [22] M. Jesussek, K. Ellermann, Fault detection and isolation for a full-scale railway vehicle suspension with multiple Kalman filters, *Veh. Syst. Dyn.* 52 (2014) 1695–1715. doi:10.1080/00423114.2014.959026.
- [23] J. Wang, Y. Peng, W. Qiao, J.L. Hudgins, Bearing Fault Diagnosis of Direct-Drive Wind Turbines Using Multiscale Filtering Spectrum, *IEEE Trans. Ind. Appl.* 53 (2017) 3029–3038. doi:10.1109/TIA.2017.2650142.
- [24] S.S. Haykin, *Neural networks and learning machines*, 3rd ed, Prentice Hall, New York, 2009.
- [25] V. Vapnik, *Estimation of Dependences Based on Empirical Data*, Springer-Verlag, New York, 2006. //www.springer.com/la/book/9780387308654 (accessed June 26, 2018).
- [26] T.J. Ross, *Fuzzy Logic with Engineering Applications*, John Wiley & Sons, 2009.
- [27] G. Marichal, M. Artés, J. García-Prada, An intelligent system for faulty-bearing detection based on vibration spectra, *J. Vib. Control*. 17 (2011) 931–942. doi:10.1177/1077546310366264.
- [28] W. Chen, W. Liu, K. Li, P. Wang, H. Zhu, Y. Zhang, C. Hang, Rail crack recognition based on Adaptive Weighting Multi-classifier Fusion Decision, *Measurement*. 123 (2018) 102–114. doi:10.1016/j.measurement.2018.03.059.
- [29] S. Braun, D.J. Ewins, S.S. Rao, eds., *Encyclopedia of vibration*, Academic Press, San Diego, 2002.
- [30] M.P. Norton, D.G. Karczub, *Fundamentals of noise and vibration analysis for engineers*, Cambridge Univ. Press, Cambridge, 2007. doi:10.1017/CBO9781139163927.
- [31] Case Western Reserve University Bearing Data Center Website, (n.d.). <http://csegroups.case.edu/bearingdatacenter/home> (accessed July 5, 2018).
- [32] W.A. Smith, R.B. Randall, Rolling element bearing diagnostics using the Case Western Reserve University data: A benchmark study, *Mech. Syst. Signal Process.* 64–65 (2015) 100–131. doi:10.1016/j.ymsp.2015.04.021.

- [33] A. Bustos Caballero, Metodología para la mejora del diseño de sistemas mecánicos de responsabilidad para el uso de tecnologías avanzadas de mantenimiento DM&M, Universidad Carlos III de Madrid, 2017. <https://e-archivo.uc3m.es/handle/10016/26298>.